
Proceedings Paper:
Alsharkawi, A. and Rossiter, J.A. orcid.org/0000-0002-1336-0633 (2017) Modelling Analysis of a Solar Thermal Power Plant. In: 2017 6th International Conference on Clean Electrical Power (ICCEP). 6th International Conference on Clean Electrical Power (ICCEP), 27-29 Jun 2017, Santa Margherita Ligure, Italy. IEEE .

https://doi.org/10.1109/ICCEP.2017.8004766

Modelling Analysis of a Solar Thermal Power Plant

A. Alsharkawi*, J.A. Rossiter**
Department of Automatic Control and Systems Engineering
University of Sheffield
Sheffield, S1 3JD, UK
Email: *aalsharkawi1@sheffield.ac.uk, **j.a.rossiter@sheffield.ac.uk

***Abstract*—This paper looks into the modelling of the ACUREX distributed solar collector field at the Plataforma Solar de Almería (PSA). ACUREX possesses resonance characteristics that lie well within the desired control bandwidth and quite commonly is modelled by dividing the receiver tube in the solar collector field into a number of segments. However, the number of segments has varied significantly in the literature. This paper provides an open-loop and closed-loop analysis with the aim of finding the number of segments needed to adequately model the resonance characteristics.**

***Index Terms*—Nonlinear systems, Parabolic trough, Resonant modes, Solar thermal power plant.**

I. Introduction

A. Background and problem statement

The latest world energy statistics [1] illustrate the need to produce marketable electricity from clean and sustainable alternatives to fossil fuels. The steady increase in the consumption of fossil fuels (coal, oil and natural gas) and their contribution to CO_2 emissions are the driving factors behind this need. Solar energy is a highly appealing alternative.

In 2011, the International Energy Agency (IEA) stated that "The development of affordable, inexhaustible and clean solar energy technologies will have huge longer-term benefits. It will increase countries' energy security through reliance on an indigenous, inexhaustible and mostly import-independent resource, enhance sustainability, reduce pollution, ... " [2].

Solar energy is converted into electrical energy by two main approaches; a direct approach using photovoltaic (PV) technology and an indirect approach using concentrated solar power (CSP) technology, where electricity is produced by thermal means [3]. The scope of this paper will be limited to the application of the most developed CSP technology, namely parabolic trough.

ACUREX is a parabolic trough technology-based solar thermal power plant. It is one of the research facilities of the Plataforma Solar de Almería (PSA) in south-east Spain and has served as a benchmark for many researchers across academia and industry. Collectors of the ACUREX plant are parabolic in shape and concentrate the incident solar radiation onto a receiver tube that is placed at its focal line. A heat transfer fluid (HTF) is heated as it flows through the receiver tube and circulates through a distributed solar collector field. The heated HTF then passes through a series of heat exchangers to produce steam which in turn is used to drive a steam turbine to generate electricity.

From a control point of view, one of the biggest challenges is to maintain the field outlet temperature at a desired level despite changes, mostly in solar radiation, field inlet temperature, or ambient temperature. This can be handled by manipulating the volumetric flow rate of the HTF. A detailed description of the plant and control problem can be found in [4].

It was argued in [5] that the ACUREX distributed solar collector field possesses resonance characteristics, namely resonant modes that lie well within the desired control bandwidth. These phenomena arise due to the relatively slow flow rate of the HTF and the length of the receiver tube. It was also found that the phenomena have a significant impact on the control performance and hence modelling the resonant modes sufficiently accurately is crucial to ensure high control performance with adequate robustness.

A common approach for constructing nonlinear models of the ACUREX plant is to divide the receiver tube in the solar collector field into a number of segments as will be discussed later on in the paper. However, the literature has witnessed a significant variation in the number of segments used and hence it makes one wonder how many segments are actually needed to adequately model the resonant modes of the plant. Surprisingly, this has received little attention in the literature.

B. Paper contribution and organisation

The paper draws attention to a practice that can be helpful in deciding on the number of segments needed and hence begins by constructing a number of nonlinear simulation models of the plant for a different number of segments and investigating their performance in an open-loop and closed-loop fashion.

For the open-loop analysis, the performance of each model will be analysed against a measured output from the ACUREX plant. The closed-loop analysis requires the estimation of a linear time-invariant (LTI) state space model from each and every constructed nonlinear simulation model and hence the estimation process and some frequency-domain analysis will be discussed first.

A brief literature review of the available nonlinear models of the ACUREX plant is presented in Section II and then a general procedure for constructing a nonlinear simulation model for any number of segments is discussed in Section III. This is followed by an open-loop analysis in Section IV and Closed-loop analysis in Section V. Finally, Section VI is devoted to a discussion of the overall results and some concluding remarks.

II. Nonlinear models of the ACUREX plant

The dominant dynamics of the ACUREX plant are captured by a set of energy balance partial differential eqns. (PDEs):

$$\begin{array}{l}\rho_m C_m A_m \frac{\partial T_m}{\partial t} = n_o G I - D_o \pi H_l (T_m - T_a) \\ -D_i \pi H_t (T_m - T_f) \\ \rho_f C_f A_f \frac{\partial T_f}{\partial t} + \rho_f C_f q \frac{\partial T_f}{\partial x} \\ = D_i \pi H_t (T_m - T_f)\end{array} \quad (1)$$

where the subindex m refers to the metal of the receiver tube and f to the HTF [4], [6]. See Table I for variables and parameters.

TABLE I: Variables and Parameters.

Symbol	Description	SI unit
ρ	Density	kg/m^3
C	Specific heat capacity	J/kg°C
A	Cross-sectional area	m^2
T	Temperature	$^\circ$C
t	Time	s
I	Solar radiation	W/m^2
n_o	Mirror optical efficiency	$-$
G	Mirror optical aperture	m
D_o	Outer diameter of the receiver tube	m
H_l	Global coefficient of thermal losses	W/m°C
T_a	Ambient temperature	$^\circ$C
D_i	Inner diameter of the receiver tube	m
H_t	Coefficient of metal-fluid heat transfer	$W/m^{2\circ}$C
q	HTF volumetric flow rate	m^3/s
x	Space	m

It is a common practice in the literature to construct nonlinear simulation and prediction models based on these PDEs by dividing the receiver tube into N segments each of length Δx and then converting the set of PDEs (1) into a set of ordinary differential equations (ODEs) or simply a set of difference equations. One of the early constructed nonlinear simulation models is reported in [4], where the receiver tube was divided into 100 segments each of length $1m$. The PDEs (1) were solved using a two-stage algorithm of three difference equations.

More recently and after simplifying the PDEs by neglecting the dynamics of the metal of the receiver tube, a set of ODEs has been obtained for simulation and prediction purposes. For simulation purposes, the receiver tube was divided into 10 segments and for prediction purposes and after neglecting the heat losses, the receiver tube was divided into 5 segments [7]. In [8], in an attempt to obtain a linearised state space model of the plant, an ODE is obtained from a simplified version of the PDEs and the receiver tube has been divided into 8 segments whereas in [9] and for the same exact reason, the PDEs were converted into a set of ODEs by dividing the receiver tube into 15 segments.

Clearly, the number of segments used to construct nonlinear simulation and prediction models has varied significantly (from 5 to 100) in the literature and these are examples where the number of segments was stated explicitly.

III. Construction of a nonlinear simulation model

The set of PDEs (1) can be approximated by a set of ODEs by dividing the receiver tube into "N" segments each of length Δx with the boundary condition $T_{f,0} = T_{f,inlet}$ (field inlet temperature) and H_l,H_t,ρ_f and C_f being time−varying [10].

$$\begin{array}{l}\rho_m C_m A_m \frac{dT_{m,n}}{dt} = n_o G I \\ -D_o \pi H_l (T_{m,n} - T_a) \\ -D_i \pi H_t (T_{m,n} - T_{f,n}) \\ \rho_f C_f A_f \frac{dT_{f,n}}{dt} + \rho_f C_f q \frac{T_{f,n} - T_{f,n-1}}{\Delta x} \\ = D_i \pi H_t (T_{m,n} - T_{f,n})\end{array} \quad , \quad n = 1, ..., N \quad (2)$$

The set of ODEs (2) is transparent and can be simply implemented for any number of segments. In order to meet the first aim of this paper, five nonlinear simulation models have been constructed for $N = 15$, 13, 10, 7, and 4.

Remark 1. *The set of ODEs (2) is implemented and solved for the five nonlinear simulation models using the MATLAB solver ODE45 (an explicit Runge-Kutta method) where the temperature distribution in the receiver tube and HTF can be accessed at any point in time and for any segment n. The number of ODEs solved at each sample time k for a nonlinear simulation model of N segments is $2 \times N$.*

IV. Open-loop analysis

In this section and using some measured data † from the ACUREX plant, the performance of the five nonlinear simulation models is assessed in the time-domain and in an open-loop manner. Fig. 1 shows the measured inputs and Fig. 2 shows the performance of the five nonlinear simulation models against the measured output. Note that models 1, 2, 3, 4 and 5 refer to the nonlinear simulation models with 15, 13, 10, 7 and 4 segments respectively.

Inspection of Fig. 2 indicates that the variation in the number of segments is only affecting the transients, i.e., the larger the number of segments the slower the response. To gain better insight into the respective performance, Table II gives a numerical comparison of the five non-linear models.

TABLE II: Assessment of the Simulation Models

Simulation model	RMSE ($^\circ$C)
1	14.4859
2	14.2301
3	13.8792
4	13.5739
5	13.3112

Table II shows that a small number of segments gives lower root mean square error (RMSE), but the impact on RMSE of the variation in the number of segments is not significant. The similarity in accuracy of these models could be an explanation for the notable variation in the number of segments used in the literature; the next section delves deeper into the problem.

†The measured data was collected on 15 July 2003 and after a series of step changes in the volumetric flow rate of the HTF.

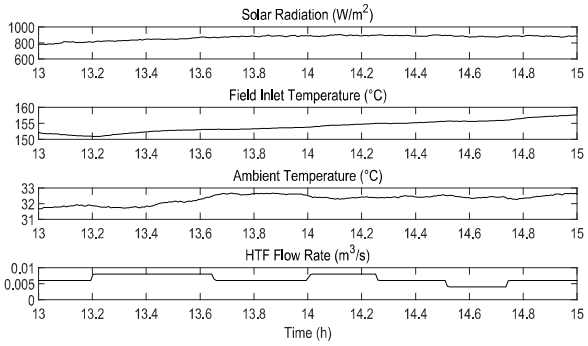

Fig. 1: Measured inputs.

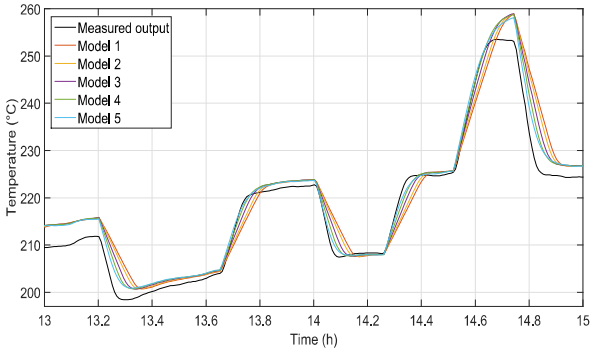

Fig. 2: Simulation models against the measured output.

V. Closed-loop analysis

A. Control objective and strategy

It has been mentioned earlier that in a solar thermal power plant a core control objective is to keep the field outlet temperature at a specific target in spite of any changes in solar radiation, the field inlet temperature, or ambient temperature by suitably adjusting the volumetric flow rate of the HTF. In order to meet this aim, researchers have proposed many different control strategies (e.g. see comprehensive surveys on control strategies [11], [12]).

In [10], and due to the nonlinearity of the ACUREX plant, a predictive control strategy has been designed locally around a single operating point. That control strategy is adopted here and used to investigate the performance of the five nonlinear simulation models. The control strategy is model-based and hence a local LTI state space model needs to be estimated from each of the five nonlinear simulation models.

B. System identification and frequency-domain analysis

Following the same identification process in [10], LTI state space models are estimated directly from input-output data using the subspace identification method N4SID [13]. Table III gives a summary of the results. Local models 1, 2, 3, 4 and 5 have been estimated from the constructed nonlinear simulation models with 15, 13, 10, 7 and 4 segments respectively.

TABLE III: Summary of the Estimated Local Models

Local model	Model order	Best fit (%)	CT (s)	MSE
1	5^{th}	97.17	125.835	0.2854
2	5^{th}	97.21	106.471	0.2649
3	5^{th}	97.21	79.556	0.2373
4	4^{th}	97.16	53.797	0.212
5	3^{rd}	97.10	30.443	0.1909

One way of describing Table III is to say that as the number of segments is increased, the model order of the estimated state space models is increased as well as the computational time (CT) required to obtain the input-output data. The best fit and mean squared error (MSE) are quantitative assessments of the estimation process and one can notice slight variation to their values. For more details about the model order selection and the best fit criterion, readers are referred to [10].

The fact that the time-domain analysis gives little information about the resonant modes of the plant necessitated an alternative approach. Fig. 3 shows the frequency response of the locally estimated LTI state space models. The Bode plot clearly shows that the resonant modes indeed lie within the Nyquist bandwidth and more importantly, as the number of segments is increased they become more obvious and indeed the resonance characteristics are not quite captured by local model 5.

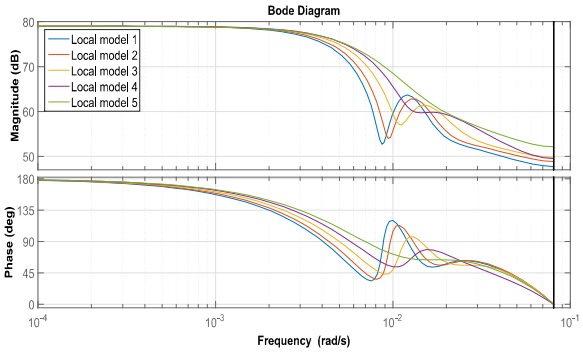

Fig. 3: Frequency response of the estimated local models.

C. Simulation results

The estimated local LTI state space models are used for the design of corresponding local predictive controllers. The performance of the estimated models in capturing locally the behaviour of the plant is put to the test using the simulation scenario illustrated in Fig. 4 and Fig. 5. The scenario assumes a fixed field inlet and ambient temperature and each time a local controller is applied the plant is represented by the corresponding nonlinear simulation model. The scenario starts with a clear day and slowly time-varying solar radiation, but adds a sudden drop in solar radiation at 12.45 h to simulate a passing cloud.

The closed-loop performance of the five local controllers can be summarised by the following interesting observations.

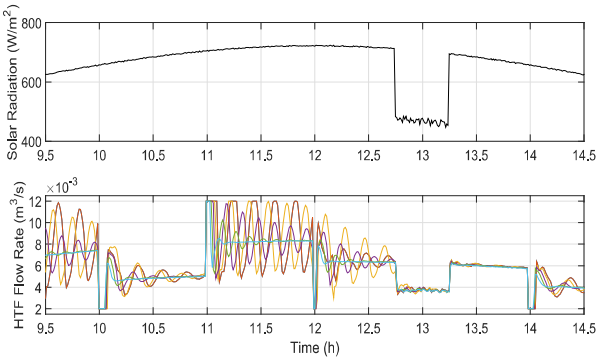

Fig. 4: Solar radiation and flow rate of the HTF.

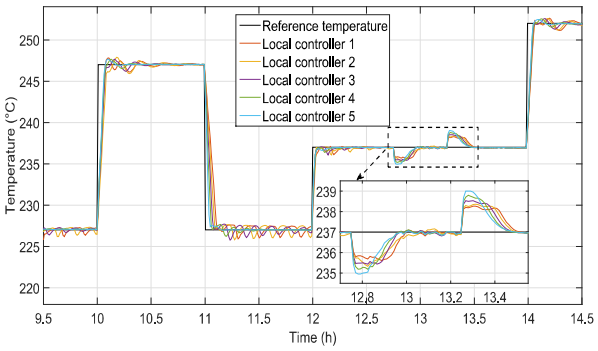

Fig. 5: Closed-loop performance.

During set point tracking, the local controllers that have been designed based on a small number of segments show less oscillatory tracking performance than the ones that have been designed based on a large number of segments. Also local controllers designed based on a large number of segments and when operating far from the nominal operating point (0.006 m^3/s) give more severe control actions.

Conversely, in terms of the resonant modes of the plant, they have been excited by the sudden drop in the solar radiation. Inspection of Fig. 5 shows that the local controllers that have been designed based on a large number of segments react to the disturbance in a better way than the ones designed based on a small number of segments.

For a better insight into the set point tracking performance and disturbance rejection, Table IV gives an assessment of the five local controllers across the whole range of operation (RMSE$_w$) and the narrow range of the disturbance (RMSE$_d$).

TABLE IV: Assessment of the Local Controllers

Local Controller	RMSE$_w$ (°C)	RMSE$_d$ (°C)
1	2.3623	0.7753
2	2.4044	0.8047
3	2.1531	0.8385
4	1.9699	0.8725
5	1.8117	0.8943

VI. Discussion and Concluding Remarks

This paper investigated the number of segments needed to adequately model the resonance characteristics of the ACUREX plant. A number of nonlinear simulation models were constructed and their performance assessed in open-loop and closed-loop manner.

The open-loop analysis revealed that the variation in the number of segments primarily affects transients and gives little information about the resonant modes. A closed-loop analysis requires the estimation of a LTI state space models; here the resonant modes are more obvious when the models are estimated from a nonlinear simulation model with many segments.

The LTI state space models were evaluated using a nonlinear simulation environment. The state space models estimated based on a large number of segments react to a sudden disturbance in a better way than those based on a small number of segments. On the other hand, the state space models estimated based on a small number of segments have shown better set point tracking performance.

This leads to the following interesting finding. Constructing a nonlinear simulation model using a large number of segments captures the dynamics of the plant at high frequencies and constructing a nonlinear simulation model using a small number of segments captures the dynamics of the plant at low frequencies. Obviously this is a dilemma that calls for something beyond the time-based measurements to validate a nonlinear simulation model.

One way of resolving the dilemma is to relate to the frequency response of the plant. In [14], the frequency response of the plant has been obtained around three different operating points and by inspecting the frequency response of the five nonlinear simulation models around the same operating points, it has been found that a nonlinear simulation model when 7 segments are considered gives a reasonable approximation to the resonance characteristics of the plant. This can be clearly seen in Fig. 6, Fig. 7 and Fig. 8.

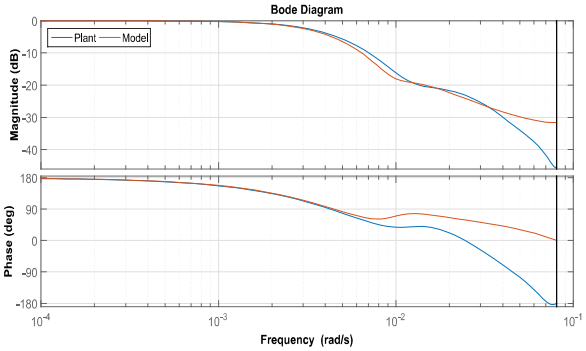

Fig. 6: Model validation around operating point 1.

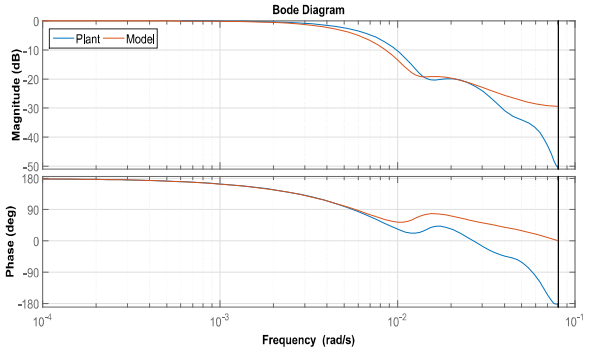

Fig. 7: Model validation around operating point 2.

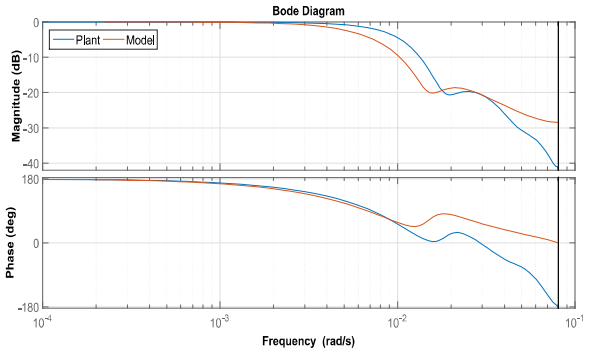

Fig. 8: Model validation around operating point 3.

Note that the linear models that have been used here to generate the frequency response of the plant are quite controversial as discussed in [15] due to the fact that these models were subject to changes in solar radiation during the identification process, but this is not an issue here since the normalised steady-state gain has been used for validation.

ACKNOWLEDGMENT

The authors would like to thank Robin De Keyser and Clara Ionescu from Ghent University, Belgium for their cooperation and providing us with measured data from the ACUREX distributed solar collector field.

REFERENCES

[1] *Key world energy statistics*. International Energy Agency, 2016.
[2] *Solar energy perspectives*. International Energy Agency, 2011.
[3] D. Y. Goswami, F. Kreith, and J. F. Kreider, *Principles of solar engineering*. CRC Press, 2000.
[4] E. F. Camacho, M. Berenguel, F. R. Rubio, and D. Martínez, *Control of solar energy systems*. Springer-Verlag, 2012.
[5] A. Meaburn and F. Hughes, "Resonance characteristics of distributed solar collector fields," *Solar Energy*, vol. 51, no. 3, pp. 215–221, 1993.
[6] R. Carmona, "Analysis, modeling and control of a distributed solar collector field with a one-axis tracking system," *Spanish: University of Seville, Spain*, 1985.
[7] M. Gálvez-Carrillo, R. De Keyser, and C. Ionescu, "Nonlinear predictive control with dead-time compensator: Application to a solar power plant," *Solar energy*, vol. 83, no. 5, pp. 743–752, 2009.
[8] A. Gallego and E. Camacho, "Adaptative state-space model predictive control of a parabolic-trough field," *Control Engineering Practice*, vol. 20, no. 9, pp. 904–911, 2012.
[9] A. Gallego, F. Fele, E. Camacho, and L. Yebra, "Observer-based model predictive control of a parabolic-trough field," *Solar Energy*, vol. 97, pp. 426–435, 2013.
[10] A. Alsharkawi and J. Rossiter, "Dual mode mpc for a concentrated solar thermal power plant," *IFAC-PapersOnLine*, vol. 49, no. 7, pp. 260–265, 2016.
[11] E. Camacho, F. Rubio, M. Berenguel, and L. Valenzuela, "A survey on control schemes for distributed solar collector fields. part i: Modeling and basic control approaches," *Solar Energy*, vol. 81, no. 10, pp. 1240–1251, 2007.
[12] ——, "A survey on control schemes for distributed solar collector fields. part ii: Advanced control approaches," *Solar Energy*, vol. 81, no. 10, pp. 1252–1272, 2007.
[13] P. Van Overschee and B. De Moor, *Subspace identification for linear systems: Theory-Implementation-Applications*. Springer Science & Business Media, 1996.
[14] T. A. Johansen, K. J. Hunt, and I. Petersen, "Gain-scheduled control of a solar power plant," *CEP*, 2000.
[15] A. Alsharkawi and J. Rossiter, "Gain scheduling dual mode mpc for a solar thermal power plant," *IFAC-PapersOnLine*, vol. 49, no. 18, pp. 128–133, 2016.